INTERNATIONAL JOURNAL OF HYDROGEN ENERGY XXX (2013) 1–7

Available online at www.sciencedirect.com

SciVerse ScienceDirect

journal homepage: www.elsevier.com/locate/he

High performance solid oxide electrolysis cells using $Pr_{0.8}Sr_{1.2}(Co,Fe)_{0.8}Nb_{0.2}O_{4+\delta}$–Co–Fe alloy hydrogen electrodes

Chenghao Yang [a,**], *Zhibin Yang* [b], *Chao Jin* [c], *Meilin Liu* [a,d], *Fanglin Chen* [e,*]

[a] *New Energy Research Institute, College of Environment and Energy, South China University of Technology, Guangzhou 510006, PR China*

[b] *Union Research Center of Fuel Cell, School of Chemical & Environment Engineering, China University of Mining & Technology, Beijing 100083, PR China*

[c] *School of Energy, Soochow University, Suzhou, Jiangsu 215006, PR China*

[d] *School of Materials Science & Engineering, Georgia Institute of Technology, Atlanta, GA 30332-0245, USA*

[e] *Department of Mechanical Engineering, University of South Carolina, 300 Main Street, Columbia, SC 29208, USA*

ARTICLE INFO

Article history:
Received 25 April 2013
Received in revised form
17 June 2013
Accepted 18 June 2013
Available online xxx

Keywords:
Solid oxide electrolysis cell
Hydrogen production
Ceramic electrode
Perovskite
Co–Fe Alloy

ABSTRACT

A novel ceramic hydrogen electrode material consisting of K_2NiF_4-type structured $Pr_{0.8}Sr_{1.2}(Co,Fe)_{0.8}Nb_{0.2}O_{4+\delta}$ (K-PSCFN) matrix with homogenously dispersed nano-sized Co–Fe alloy (CFA) has been demonstrated by annealing perovskite $Pr_{0.4}Sr_{0.6}Co_{0.2}Fe_{0.7}Nb_{0.1}O_{3-\delta}$ (P-PSCFN) in H_2 at 900 °C. Impedance spectra and voltage–current density curves of the $La_{0.8}Sr_{0.2}Ga_{0.83}Mg_{0.17}O_{3-\delta}$ (LSGM) electrolyte supported solid oxide electrolysis cell (SOEC) with a configuration of K-PSCFN–CFA/LSGM/$Ba_{0.9}Co_{0.7}Fe_{0.2}Nb_{0.1}O_{3-\delta}$ (BCFN) have been evaluated as a function of the operating temperature and feeding gas absolute humidity (AH) to characterize the cell performance. Cell polarization resistances (R_p) were as low as 0.77 and 0.31 $\Omega\,cm^2$ under open circuit voltage (OCV) and 60% absolute humidity (AH) at 800 and 900 °C, respectively. The cell has demonstrated good stability for high temperature stream electrolysis, and a hydrogen production rate of 707 $ml/cm^2\,h$ calculated from the Faraday's law has been achieved under an electrolysis voltage of 1.3 V and 60 vol.% AH at 900 °C. The cell performance results indicate that K-PSCFN–CFA is a promising hydrogen electrode for high temperature solid oxide electrolysis cells.

1. Introduction

Increasing reliance on finite fossil fuels has recently highlighted energy and environmental concerns. Hydrogen has been considered to be a leading candidate as secondary energy carrier due to its clean, storable and environmental benign characteristics. Hydrogen production has been primarily based on steaming reforming of natural gas, but it is not a sustainable process since it consumes fossil fuels and releases large quantities of greenhouse gases to the

* *Corresponding author.* Tel.: +1 803 777 4875.
** *Corresponding author.*
E-mail addresses: esyangc@scut.edu.cn (C. Yang), chenfa@cec.sc.edu (F. Chen).

0360-3199/$ – see front matter Copyright © 2013, Hydrogen Energy Publications, LLC. Published by Elsevier Ltd. All rights reserved.
http://dx.doi.org/10.1016/j.ijhydene.2013.06.086

atmosphere [1,2]. The prospect of hydrogen economy requires the development of clean and efficient hydrogen generation approaches. High temperature electrolysis of steam via solid oxide electrolysis cells (SOECs) has been attracting much attention since hydrogen production can be efficiently achieved from water splitting at high temperature from both thermodynamic and kinetic perspectives [3–6]. Furthermore, high temperature electrolysis of steam can take advantage of the heat supplies from the next generation nuclear plant as well as the waste heat from the high temperature industrial process and electrical power supplied by renewable energy such as solar, wind, tidal and geothermal sources, potentially offering an efficient option for large scale and high-purity hydrogen production [7,8].

SOEC is in principle a reversible process of solid oxide fuel cell (SOFC), and it can be operated efficiently both in SOEC mode for hydrogen generation through steam electrolysis and in SOFC mode for electricity generation by electrochemically combining fuel with oxidant [5,6,9]. Compared to secondary batteries and ultra-capacitors, reversible SOEC (RSOEC) is an ideal and cost effective device for energy storage and conversion, and it can take advantage of excess electrical capacity in the grid during off-peak hours to produce hydrogen and then utilize it later during period of high electrical power demand. Therefore, research of high temperature electrolysis of steam for hydrogen production via SOEC is mainly based on the experiences accumulated in the SOFC studies for achieving high and durable cell performance. Ni–yttria stabilized zirconia (YSZ) has been extensively used as SOEC hydrogen electrode due to its excellent catalytic properties at elevated operating temperatures, good electronic conductivity as well as closely-matched thermal expansion behavior to the electrolyte. However, studies have demonstrated that Ni–YSZ hydrogen electrode has suffered silica segregation and irreversible degradation in high steam concentrations or low hydrogen partial pressure, and the Ni particles seem to be coarsened and oxidized [10–13]. Therefore, it is necessary to find a more stable, nickel free and highly active SOEC hydrogen electrode. Studies have demonstrated that perovskite $(La_{0.75}Sr_{0.25})_{0.95}Cr_{0.5}Mn_{0.5}O_3$ (LSCM) [14] and $Sr_2Fe_{1.5}Mo_{0.5}O_{6-\delta}$ (SFM) [15] can be potentially used as SOEC hydrogen electrode materials. The LSCM and SFM could work in high steam concentration with low content of H_2 or without H_2, and considerable performance improvement has been obtained compared to Ni-based electrodes in low hydrogen concentration conditions. However, there have been very limited reports of Ni-free ceramic materials as potential SOEC hydrogen electrode, and future study is therefore needed.

In this study, we report a novel composite hydrogen electrode material consisting of K_2NiF_4-type structured $Pr_{0.4}Sr_{0.6}(Co,Fe)_{0.4}Nb_{0.1}O_{4+\delta}$ (K-PSCFN) matrix with homogenously dispersed nano-sized Co–Fe alloy (CFA). This composite hydrogen electrode material is obtained by annealing perovskite $Pr_{0.4}Sr_{0.6}Co_{0.2}Fe_{0.7}Nb_{0.1}O_{3-\delta}$ (P-PSCFN) in H_2 at 900 °C. The K-PSCFN–CFA composite hydrogen electrode has demonstrated similar catalytic activity for steam electrolysis to Ni-based SOEC hydrogen electrode.

2. Experimental

2.1. Electrode materials and solid oxide electrolysis cells fabrication

$Pr_{0.4}Sr_{0.6}Co_{0.2}Fe_{0.7}Nb_{0.1}O_{3-\delta}$ (P-PSCFN) powders were fabricated with a solid-state reaction method. Stoichiometric amount of raw materials $Pr(NO_3)_3{\cdot}6H_2O$, $SrCO_3$, $Co(NO_3)_2{\cdot}6H_2O$, Fe_2O_3 and Nb_2O_5 were mixed by ball milling in alcohol for 24 h to prepare the P-PSCFN precursor powders. The precursor powders were then dried under infrared lamp and calcined in air at 1050 °C for 5 h to obtain pure P-PSCFN phase. The $La_{0.8}Sr_{0.2}Ga_{0.83}Mg_{0.17}O_{3-\delta}$ (LSGM) electrolyte powders and $Ba_{0.9}Co_{0.7}Fe_{0.2}Nb_{0.1}O_{3-\delta}$ (BCFN) oxygen electrode powders were also fabricated by a solid-state reaction method [16]. LSGM electrolyte supported single cells with the cell configuration of K-PSCFN–CFA/LSGM/BCFN were studied in this work. The LSGM electrolyte substrates were fabricated by dry-pressing LSGM powder uniaxially under 200 MPa, followed by sintering in air at 1450 °C for 10 h. The electrode ink consisting of P-PSCFN or BCFN powders and binder (Heraeus V-006) was applied to the surface of the sintered LSGM pellet by the screen-printing method, and then fired in air at 1000 °C for 2 h. The obtained electrolysis button cell has ~12 mm in diameter, 0.33 cm^2 in oxygen electrode area, ~60 μm in thickness of the K-PSCFN–CFA hydrogen electrode layer, ~300 μm in thickness of the LSGM membrane electrolyte, and ~20 μm thickness of the BCFN oxygen electrode layer. To avoid potential catalytic influence on the hydrogen electrode reaction, Au slurry was printed on the surface of the hydrogen electrode as current collector. Pt slurry was printed on the surface of the oxygen electrode as current collector.

2.2. Characterization

The powder X-ray diffraction (XRD) pattern was recorded on an Rigaku D/Max 2100 Powder X-ray Diffractometer with a Cu-Kα radiation ($\lambda = 1.5418$ Å), employing a scan rate of 5° min^{-1} in the 2θ range from 20° to 80°. The microstructure of the powders and cell electrodes were characterized using a field emission scanning electron microscope (FESEM, Zeiss Ultra plus).

The high temperature electrolysis cell testing system is assembled according to the schematic diagram shown in Fig. 1 [5,6,17]. High temperature electrolysis testing system includes major components such as gas supply, delivery and control elements (gas cylinders, pressure regulators and mass flow controllers), steam generation and monitoring elements (humidifier and humidity sensors), temperature measurement, high temperature furnace, solid oxide electrolysis button cells, and electrochemical testing equipment (potentiostat/galvanostat and impedance response analyzer). Button cells were sealed to one end of an alumina tube with a ceramic paste (Aremco-552), and heated up to 800 °C in air. At 800 °C, prior to the flow of H_2 to the hydrogen electrode, N_2 was used to purge the hydrogen electrode side. The cell was then heated up to 900 °C and dwelled for 2 h to have the P-PSCFN anode fully annealed. The cells were subsequently cooled down to 750–850 °C and the electrochemical testing was performed.

Please cite this article in press as: Yang C, et al., High performance solid oxide electrolysis cells using $Pr_{0.8}Sr_{1.2}(Co,Fe)_{0.8}Nb_{0.2}O_{4+\delta}$–Co–Fe alloy hydrogen electrodes, International Journal of Hydrogen Energy (2013), http://dx.doi.org/10.1016/j.ijhydene.2013.06.086

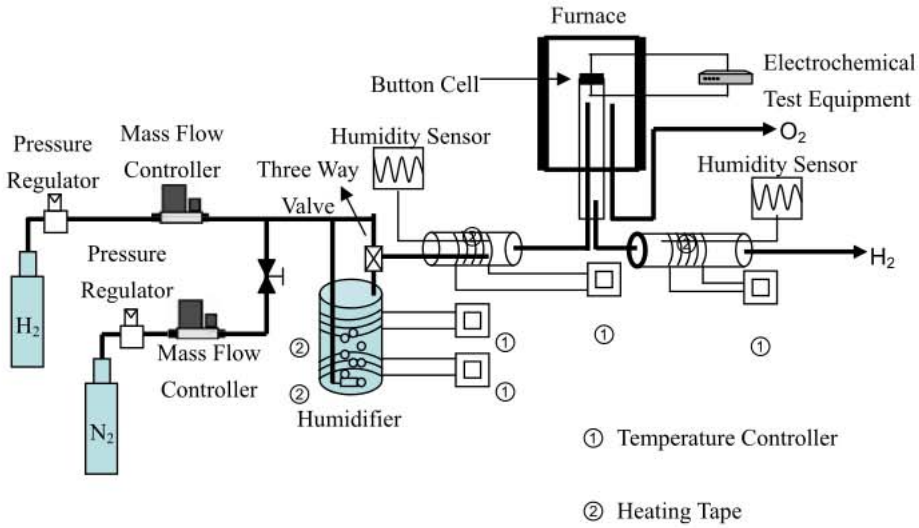

Fig. 1 – Schematic of experimental setup for high temperature electrolysis cell measurements.

The current density–voltage curves as well as the electrochemical impedance spectra (EIS) were measured with a multi-channel VersaSTAT (Princeton Applied Research). The EIS spectra were typically measured in the frequency range from 0.01 Hz to 1 MHz. All the cells were first conditioned at a constant current density with H_2 flowing to the hydrogen electrode chamber to obtain steady state performance before switching to the SOEC test. In the SOEC mode, hydrogen was used as an inlet carrier gas in the hydrogen electrode to control the partial pressure of the steam. Hydrogen flow rate was controlled by a precision mass flow controller (Alicat Scientific). Hydrogen was mixed with water vapor using a humidifier. The amount of water vapor in the gas mixture was continuously measured in term of absolute humidity (AH, the vol.% of humidity in the total gas volume) using an on-line humidity sensor (Vaisala Model HMP 337). With each AH value at a given temperature, the water vapor flow rate is proportional to the hydrogen carrier gas flow rate. The humidity sensor was located downstream of the humidifier housed in a stainless steel assembly. Hydrogen generation rate of the SOEC was calculated from the Faraday's law, assuming a 100% current efficiency based on the experimental results reported by O'Brien et al. [5,6].

3. Results and discussion

3.1. *Materials characterization and electrode microstructure*

Fig. 2A shows the X-ray diffraction (XRD) patterns of P-PSCFN powders before and after reduction in H_2 at 900 °C for 2 h. XRD patterns indicate that after reduction in H_2 at 900 °C for 2 h the P-PSCFN powders are fully transformed into a K-PSCFN and CFA mixture, and therefore the cell hydrogen electrode is actually K-PSCFN and CFA composite instead of P-PSCFN. Fig. 2B shows the cross-sectional SEM image of the LSGM electrolyte-supported single cell after over 200 h SOFC/SOEC testing, and good adhesion is observed in the porous electrodes and the dense LSGM electrolyte interfaces. It has been well established that the electrode electrochemical reaction typically happens at the electrode three phase boundaries (TPBs), and the length of electrode TPBs can be significantly influenced by the porous electrode morphology [18,19]. Therefore, the microstructure of the hydrogen and oxygen electrodes has been examined. As shown in Fig. 2(C and D), the hydrogen and oxygen electrodes are composed of porous network well attached to the LSGM electrolyte. Fig. 2E shows that the nano-sized CFA particles are homogenously dispersed on the K-PSCFN matrix in the K-PSCFN–CFA hydrogen electrode after over 200 h high temperature (800–900 °C) SOFC/SOEC tests.

3.2. *Impedance study*

Fig. 3 a, b and c) shows the impedance spectra of the SOECs with the configuration of K-PSCFN–CFA/LSGM/BCFN measured as a function of operating temperature and different steam concentration in the feeding gas stream under open circuit voltage (OCV) conditions. The cell impedance spectra were further evaluated by fitting impedance data with the equivalent circuit shown in Fig. 3d. L is the inductance, which could be due to the platinum current/voltage probes or the high-frequency phase shift of the electrochemical equipment, R_o in the circuit describes the ohmic resistance attributed from the electrolyte and lead wires, (R_1; CPE_1) and (R_2; CPE_2) correspond to the high- and low-frequency arcs, respectively. The influence of the operating temperature on the cell performance can be clearly seen. Both the cell R_o and area specific resistance (ASR) decreased with the increase of the cell operating temperature. The influence of the feeding gas humidity on cell performance reveals that the increase in the feeding gas humidity leads to an increase in the ASR, typically from 0.54 Ω cm^2 under 20 vol.% AH to 0.77 Ω cm^2 under 60 vol.% AH at 800 °C, and from 0.23 Ω cm^2 under 20 vol.% AH to 0.31 Ω cm^2 under 60 vol.% AH at 900 °C, as

Please cite this article in press as: Yang C, et al., High performance solid oxide electrolysis cells using $Pr_{0.8}Sr_{1.2}(Co,Fe)_{0.8}Nb_{0.2}O_{4+\delta}$–Co–Fe alloy hydrogen electrodes, International Journal of Hydrogen Energy (2013), http://dx.doi.org/10.1016/j.ijhydene.2013.06.086

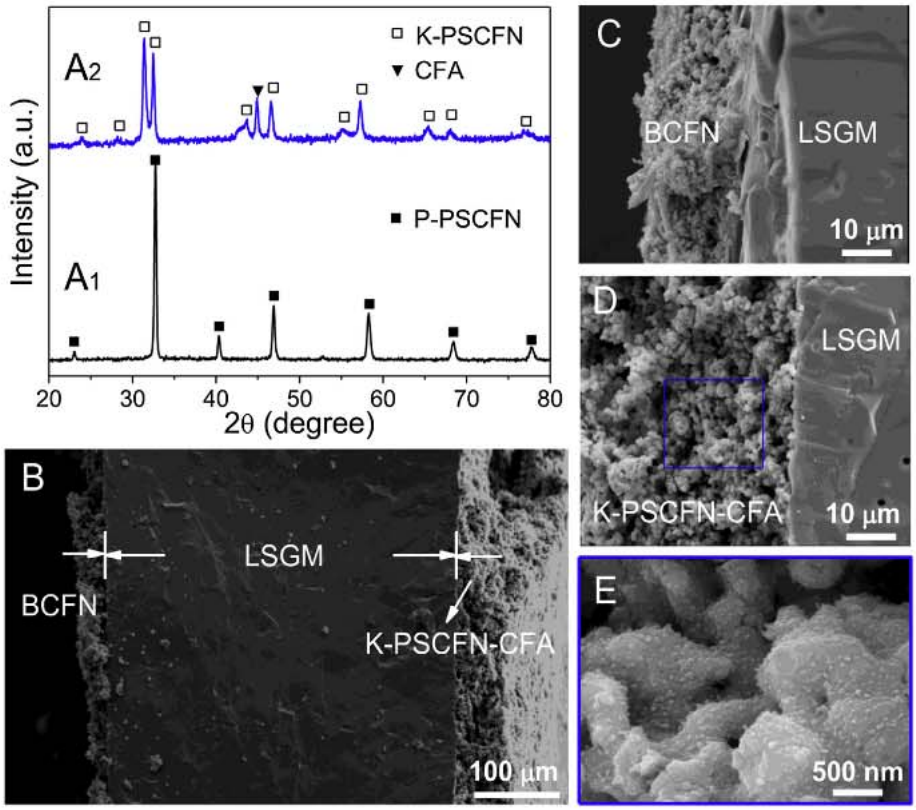

Fig. 2 – A) X-ray diffraction patterns of A1) P-PSCFN sintered in air at 1050 °C for 10 h and A2) P-PSCFN reduced in H_2 at 900 °C for 2 h, B) Cross-sectional SEM image of the LSGM electrolyte-supported solid oxide cell with K-PSCFN–CFA as hydrogen electrode and BCFN as oxygen electrode after fuel cell and electrolysis test, C) SEM image of the porous BCFN oxygen electrode on the LSGM electrolyte, D) Microstructure of the porous K-PSCFN–CFA hydrogen electrode on the LSGM electrolyte, and (E) high-magnification SEM image of the K-PSCFN–CFA hydrogen electrode after the electrochemical performance test.

shown in Figs. 3 and 4. However, the R_o was unaffected by the increase in the feeding gas AH, demonstrating that R_o is only temperature sensitive, while ASR includes considerable contributions coming from the electrode process, for example activation and concentration polarization resistance.

3.3. *Polarization study*

The electrochemical performance of the cell was further investigated through the voltage–current density curves in both SOEC and SOFC modes with different steam concentration in the feeding gas (20, 40 and 60 vol.% AH) at 800, 850 and 900 °C, respectively. The data were acquired by increasing the potential from 0.3 to 1.5 V with a 20 mV/s voltage sweep rate, and the applied cell potentials are plotted as a function of current density. Positive current densities indicate power generation (SOFC mode) while negative current densities indicate power consumption (SOEC mode). As presented in Fig. 5, the cell voltage value at zero current density corresponds to OCV, which is influenced by the steam to hydrogen ratio, and decreases with the increase of the steam to hydrogen ratio, as predicted from the Nernst Equation for the hydrogen–oxygen–steam system [17,18]. In the SOEC mode, a current density value of 0.6 A/cm^2 is observed for 20 vol.% AH with an applied cell voltage of 1.3 V, while it increases to 0.85 A/cm^2 at 60 vol.% AH at 800 °C, as shown in Fig. 5a. Relatively high current densities of 1.18 and 1.57 A/cm^2 have been achieved at 60 vol.% AH when the operating temperature is increased from 800 to 850 and 900 °C, respectively, as shown in Fig. 5b and c. Meanwhile, it is noticed that the cell applied voltage varies linearly with the current density up to a value that depends on the inlet steam concentration. For 800 °C, the voltage begins to increase exponentially at relatively lower current density for lower AH, which is ascribed to the steam starvation in electrode reaction zone due to the mass transport limitation in porous hydrogen electrode. However, the mass transport limitation is mitigated for higher AH. Similar results occur when the temperature is raised to 850 and 900 °C, but the mass transport limitation occurs even at 60 vol.% AH, indicating that the cell performance can be further improved by optimizing the porous hydrogen electrode microstructure to enhance steam transport and diffusion in the hydrogen electrode.

The hydrogen generation rate is related to current applied to the SOEC cell during the electrolysis process and could be determined through the Faraday's law as follows:

$$m = \frac{sMIt}{nF} \quad (1)$$

Please cite this article in press as: Yang C, et al., High performance solid oxide electrolysis cells using $Pr_{0.8}Sr_{1.2}(Co,Fe)_{0.8}Nb_{0.2}O_{4+\delta}$–Co–Fe alloy hydrogen electrodes, International Journal of Hydrogen Energy (2013), http://dx.doi.org/10.1016/j.ijhydene.2013.06.086

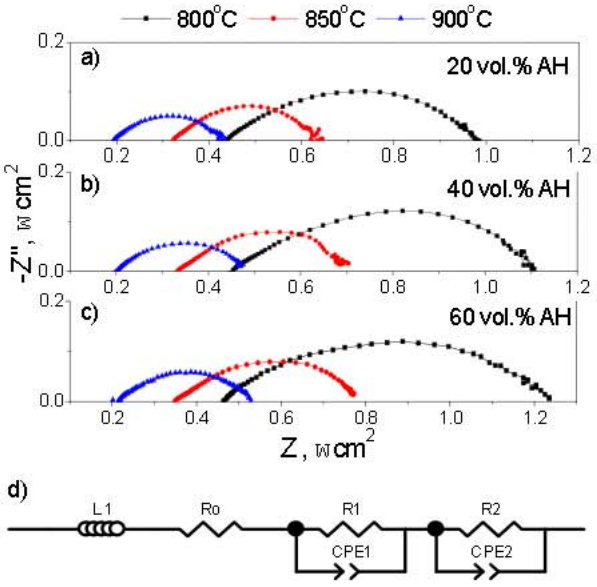

Fig. 3 – (a–c) Impedance spectra of K-PSCFN–CFA/LSGM/BCFN single cell recorded under open circuit conditions as a function of operating temperature and feeding gas absolute humidity (AH) and (d) the proposed equivalent circuit to fit the impedance spectra.

where m is the mass of the substance, s is the stoichiometric coefficient of the species, M is the atomic or molecular weight, I (A) is the current, t (s) is the time elapsed, and n is the number of the electrons involved in the charge transfer reaction. Therefore, the outlet hydrogen flow rate can be described as follows:

$$N_{H_2,p} = 60 * 10^3 \frac{sMIV_{std}}{nF} \quad (2)$$

where $N_{H_2,p}$ is outlet hydrogen mass flow rate (sccm), V_{std} (L/mol) is volume of 1 mol gas at standard temperature and pressure.

Representative plots of hydrogen production rate during DC sweeping of 60 vol.% AH at 800 and 900 °C, respectively, are shown in Fig. 6. The left hand side vertical scale is in standard

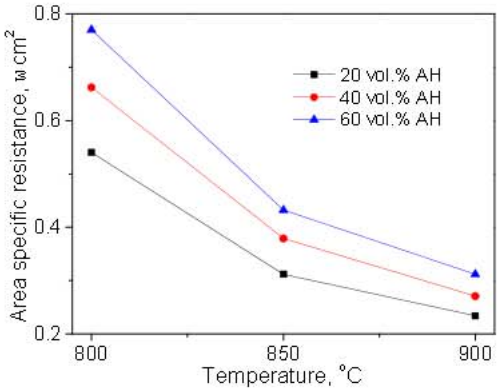

Fig. 4 – The SOEC area specific resistance (ASR) as function of the operating temperature and feeding gas AH determined from the impedance spectra.

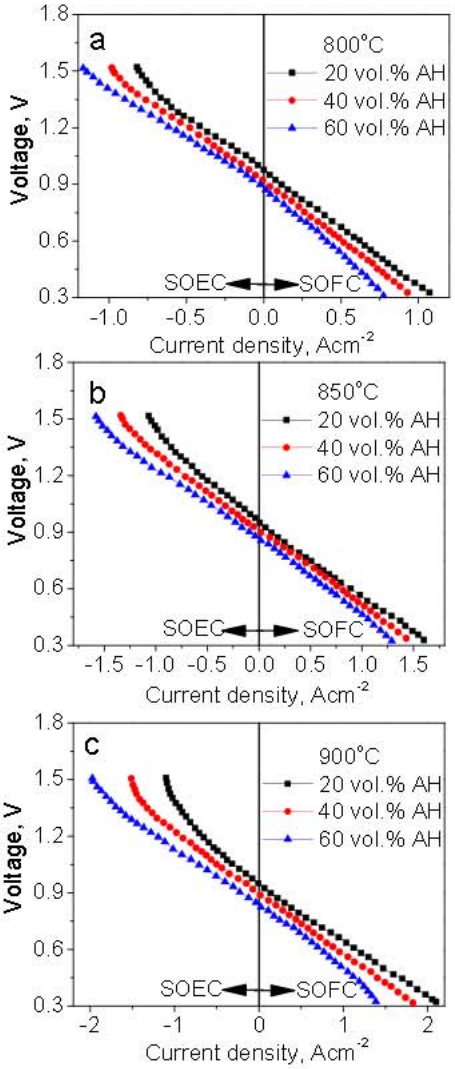

Fig. 5 – Voltage–current density curves of K-PSCFN–CFA/LSGM/BCFN cell with different AH operated under SOEC and SOFC modes at 800, 850 and 900 °C, respectively.

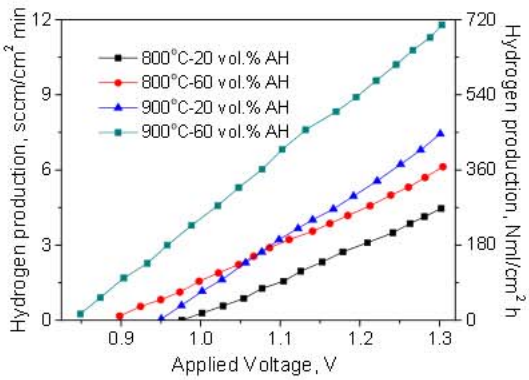

Fig. 6 – Hydrogen production rate of K-PSCFN–CFA/LSGM/BCFN single cell operated under different AH at 800 and 900 °C.

Please cite this article in press as: Yang C, et al., High performance solid oxide electrolysis cells using $Pr_{0.8}Sr_{1.2}(Co,Fe)_{0.8}Nb_{0.2}O_{4+\delta}$–Co–Fe alloy hydrogen electrodes, International Journal of Hydrogen Energy (2013), http://dx.doi.org/10.1016/j.ijhydene.2013.06.086

cubic centimeters per square centimeter per minute (sccm/cm^2 min) while the right hand side vertical axis is in normal milliliters per square centimeter per hour (Nml/cm^2 h). The hydrogen production rate increases with the increase in the electrolysis voltages, the steam concentration in the feeding gas stream as well as the operating temperature of the electrolysis cell. In this work, a hydrogen production rate as high as 707 ml/cm^2 h has been achieved at 900 °C at 60 vol.% AH with an electrolysis voltage of 1.3 V, which is even higher that of the Ni–YSZ/YSZ/LSM–YSZ cell with a hydrogen production of 362 ml/cm^2 h operated under a higher AH (80 vol.% AH) at 900 °C [17], indicating that K-PSCFN–CFA is an excellent hydrogen electrode material for efficient steam electrolysis.

3.4. *Durability test*

Fig. 7 shows the short-term cell performance of the K-PSCFN–CFA/LSGM/BCFN cell operated under a 0.6 A/cm^2 constant current at 800 °C with 60 vol.% AH in the feeding gas in the electrolysis mode for over 200 h. However, due to the limited capacity of the humidifier and the humidity of the feeding gas can not be maintained at 60 vol.% AH after over 200 h test, therefore, the test has to be interrupted. As indicated in the figure, there was a slight drop in cell voltage during the initial 30 h operation, indicating that the cell was partially activated during the electrolysis process, and the polarization resistance was decreased by the application of current. Subsequently, there was no observable electrode passivation after the cell reached the steady-state operation condition, indicating that K-PSCFN–CFA is relatively stable under high temperature and high humidity electrolysis environment. Overall, the cell shows fairly stable electrolysis performance in the 200 h short-term durability test. As shown in the high magnification SEM image (Fig. 2E) after the SOEC test, the nano-sized CFA particles are homogenously dispersed on the K-PSCFN matrix in the K-PSCFN–CFA hydrogen electrode, indicating that the K-PSCFN matrix can maintain the CFA nano-particles and prevent them from coarsening at high temperature and high steam environment, consistent to the observation of the superior performance of the K-PSCNF–CAF hydrogen electrode in the SOFC mode [20].

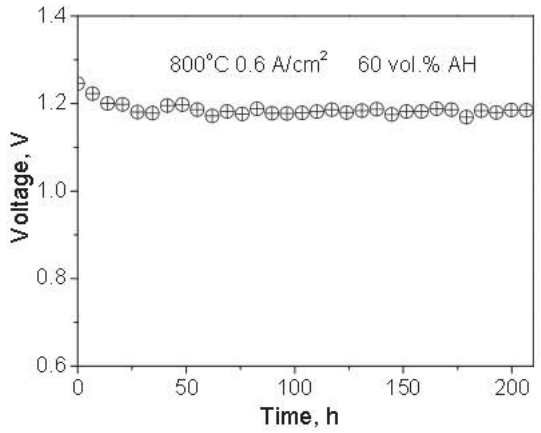

Fig. 7 – A 0.6 A/cm^2 constant current electrolysis testing of K-PSCFN–CFA/LSGM/BCFN cell at 800 °C with 60 vol.% AH.

However, for conventional Ni-based hydrogen electrode, it is well known that sintering of Ni particles will be accelerated in the presence of steam. Therefore, Ni-based electrodes are more susceptible to coarsening when the SOECs are operated at high temperature and high humidity. The agglomeration of Ni particles in Ni-based hydrogen electrode will decrease the length of the TPB where the electrode reaction taking place and lead to a fast degradation of the hydrogen electrode. This can explain the excellent stability of the K-PSCFN–CFA hydrogen electrode compared to the conventional Ni–YSZ hydrogen electrode after long-term test at high temperature (800–900 °C) and high humidity [13].

4. Conclusions

A novel ceramic hydrogen electrode material consisting of K_2NiF_4-type structured $Pr_{0.8}Sr_{1.2}(Co, Fe)_{0.8}Nb_{0.2}O_{4+\delta}$ (K-PSCFN) matrix with homogenously dispersed nano-sized Co–Fe alloy (CFA) has been obtained by annealing perovskite $Pr_{0.4}Sr_{0.6}Co_{0.2}Fe_{0.7}Nb_{0.1}O_{3-\delta}$ (P-PSCFN) in H_2 at 900 °C. The experimental investigation showed that the operating temperature and feeding gas steam concentration had significant influence on the cell performance. The impedance spectra analysis indicated that the cell R_o and R_p decreased with the increase of operating temperature, while the R_p increased with the increase in the feeding gas steam concentration. The cell showed good stability during the short-term steam electrolysis test, and a relatively high current density of 1.57 A/cm^2 was achieved at 1.3 V electrolysis voltage and 60 vol.% AH at 900 °C. This study has demonstrated that K-PSCFN–CFA is a very promising hydrogen electrode for high temperature solid oxide electrolysis cells.

Acknowledgment

The financial support of the South China University of Technology new faculty startup fund, NASA EPSCoR (Award Number NNX10AN33A) and South Carolina Space Grant Consortium is acknowledged gratefully.

REFERENCES

[1] Ming Q, Healey T, Allen L, Irving P. Steam reforming of hydrocarbon fuels. Catal Today 2002;77:51–64.
[2] Laosiripojana N, Assabumrungrat S. Conversion of poisonous methanethiol to hydrogen-rich gas by chemisorption/reforming over nano-scale CeO_2: the use of CeO_2 as catalyst coating material. Appl Catal B 2008;82:103–13.
[3] Dönitz W, Schmidberger R. Concepts and design for scaling up high temperature water vapour electrolysis. Int J Hydrogen Energy 1982;7:321–30.
[4] Hauch A, Jensen SH, Ramousse S, Mogensen M. Performance and durability of solid oxide electrolysis cells. J Electrochem Soc 2006;153:A1741–7.
[5] O'Brein JE, Stoots CM, Herring JS, Lessing PA, Hartvigsen JJ, Elangovan S. Performance measurements of solid-oxide electrolysis cells for hydrogen production. J Fuel Cell Sci Tech 2005;2:156–63.

Please cite this article in press as: Yang C, et al., High performance solid oxide electrolysis cells using $Pr_{0.8}Sr_{1.2}(Co,Fe)_{0.8}Nb_{0.2}O_{4+\delta}$–Co–Fe alloy hydrogen electrodes, International Journal of Hydrogen Energy (2013), http://dx.doi.org/10.1016/j.ijhydene.2013.06.086

[6] O'Brein JE, Stoots CM, Herring JS, Hartvigsen JJ. Hydrogen production performance of a 10-cell planar solid-oxide electrolysis stack. J Fuel Cell Sci Tech 2006;3:213–9.
[7] Herring JS, O'Brein JE, Stoots CM, Hawkes GL, Hartvigsen JJ, Shahnam M. Progress in high-temperature electrolysis for hydrogen production using planar SOFC technology. Int J Hydrogen Energy 2007;32:440–50.
[8] Ni M, Leung MKH, Leung DYC. Technological development of hydrogen production by solid oxide electrolyzer cell (SOEC). Int J Hydrogen Energy 2008;33:2337–54.
[9] Jensen SH, Larsen PH, Mogenson M. Hydrogen and synthetic fuel production from renewable energy sources. Int J Hydrogen Energy 2007;32:3253–7.
[10] Hauch A, Jensen SH, Bilde-Sorensen JB, Mogensen M. Silica segregation in the Ni/YSZ electrode. J Electrochem Soc 2007;154:A619–26.
[11] Hauch A, Ebbesen SD, Jensen SH, Mogensen M. Highly efficient high temperature electrolysis. J Mater Chem 2008;18:2331–40.
[12] Knibbe R, Traulsen ML, Hauch A, Ebbesen SD, Mogensen M. Solid oxide electrolysis cells: degradation at high current densities. J Electrochem Soc 2010;157:B1209–17.
[13] Marina OA, Pederson LR, William MC, Coffey GW, Meinhardt KD, Nguyen CD, et al. Electrode performance in reversible solid oxide fuel cells. J Electrochem Soc 2007;154:B452–9.
[14] Yang X, Irvine JTS. $(La_{0.75}Sr_{0.25})_{0.95}Mn_{0.5}Cr_{0.5}O_3$ as the cathode of solid oxide electrolysis cells for high temperature hydrogen production from steam. J Mater Chem 2008;18:2349–54.
[15] Liu Q, Yang CH, Dong XH, Chen FL. Perovskite $Sr_2Fe_{1.5}Mo_{0.5}O_{6-\delta}$ as electrode materials for symmetrical solid oxide electrolysis cells. Int J Hydrogen Energy 2010;35:10039–44.
[16] Yang ZB, Yang CH, Jin C, Han MF, Chen FL. $Ba_{0.5}Co_{0.7}Fe_{0.2}Nb_{0.1}O_{3-\delta}$ as cathode material for intermediate temperature solid oxide fuel cells. Electrochemistry Commun 2011;13:882–5.
[17] Yang CH, Coffin A, Chen FL. High temperature solid oxide electrolysis cell employing porous structured $(La_{0.75}Sr_{0.25})_{0.95}MnO_3$ with enhanced oxygen electrode performance. Int J Hydrogen Energy 2010;35:3321–6.
[18] Mizusaki J, Tagawa H, Saito T, Kamitani K, Hirano T, Ehara S, et al. Preparation of nickel pattern electrodes on YSZ and their electrochemical properties in H_2–H_2O atmospheres. J Electorochem Soc 1994;141:2129–35.
[19] Nakagawa N, Nakajima K, Sato M, Kato K. Contribution of internal active three-phase zone of Ni–zirconia cermet anodes on the electrode performance of SOFCs. J Electrochem Soc 1999;146:1290–5.
[20] Yang CH, Yang ZH, Jin C, Xiao GL, Chen FL, Han MF. Sulfur-tolerant redox-reversible anode material for direct hydrocarbon solid oxide fuel cells. Adv Mater 2012;24:1439–43.

Please cite this article in press as: Yang C, et al., High performance solid oxide electrolysis cells using $Pr_{0.8}Sr_{1.2}(Co,Fe)_{0.8}Nb_{0.2}O_{4+\delta}$–Co–Fe alloy hydrogen electrodes, International Journal of Hydrogen Energy (2013), http://dx.doi.org/10.1016/j.ijhydene.2013.06.086